

# Multi-Scale Dynamics and Rheology of Mantle Convection with Plates

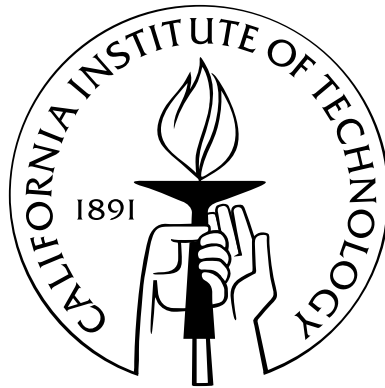
Thesis by

**Laura Alisic**

In Partial Fulfillment of the Requirements

for the Degree of

Doctor of Philosophy



California Institute of Technology

Pasadena, California

2012

(Defended April 16<sup>th</sup>, 2012)

© 2012

**Laura Alisic**

All Rights Reserved

“I do not know what I may appear to the world,  
but to myself I seem to have been only like a boy playing on the sea-shore,  
and diverting myself in now and then finding a smoother pebble or a prettier shell  
than ordinary, whilst the great ocean of truth lay all undiscovered before me.”

— *Sir Isaac Newton*

# Acknowledgements

16+ million compute hours. 122,880 compute cores. 7.2 terabytes of stored data. 6 notebooks. 5.5 years of work. These are some numbers to illustrate the effort that went into this thesis. But the real effort came from my PhD advisor, collaborators, and colleagues.

First of all, I would like to thank my advisor, Prof. Michael Gurnis, who has been a great source of inspiration and encouragement. Over the past 6 years, he has patiently taken the time to teach me how to tackle a scientific problem, how to think about and analyze numerical modeling results, and how to convey these results to peers. The latter should, after all, be the ultimate goal of a scientist. Second, I would like to thank the members of my Thesis Advisory Committee and Thesis Examination Committee for their insights and ideas: Professors Rob Clayton, Jennifer Jackson, Mark Simons, and Jean-Philippe Avouac.

This work would not have been possible without the vision, expertise, and hard work of several collaborators. The group led by Prof. Omar Ghattas in the Institute for Computational Engineering and Sciences at the University of Texas at Austin leads the pack in developing new-generation computational tools and algorithms. With the development and benchmarking of the mantle convection code `Rhea`, I have learned a tremendous amount about computational science and software development from, in particular, Georg Stadler, Carsten Burstedde, and Lucas Wilcox. The most recent component of this thesis is the modeling of past plate motions in close collaboration with Prof. Dietmar Müller's EarthByte group at the University of Sydney,

especially Kara Matthews, Nico Flament, and Maria Seton, and with Dan Bower at Caltech.

Throughout my PhD, many fruitful and stimulating scientific discussions with Dan Bower, Alejandro Soto, Erin Burkett, and Francisco Ortega have helped me more than I can say. Additionally, the technical and practical support from various people has been essential: Donna Mireles and Viola Carter in the Seismolab; Mike Black and Dian Buchness in the Department of Geological and Planetary Sciences at Caltech; and the support staff at the Texas Advanced Computing Center.

Last, and definitely not least, I would like to thank my family: my parents and my sister Eva. From a young age onward, they encouraged me to learn, explore, and be the best I can. And albeit at a distance during the past 6 years, they have provided me with an endless supply of support and a listening ear, and always showed great interest in what I was doing so far away. They give me more than anyone could ask for. A heartfelt Thank you, with a capital T.

# Abstract

Fundamental issues in our understanding of plate and mantle dynamics remain unresolved, including the rheology and state of stress of plates and slabs; the coupling between plates, slabs and mantle; the small-scale dynamics in subduction zones; the flow around slabs; and the cause of rapid changes in plate motions. To address these questions, models of global mantle flow with plates are computed using adaptive finite elements, and compared to a variety of observational constraints. These dynamically consistent instantaneous models include a composite rheology with yielding, and incorporate details of the thermal buoyancy field. Around plate boundaries, the local mesh size is 1 km, which allows us to study highly detailed features in a globally consistent framework. Models that best fit plateness criteria and plate motion data have strong slabs with high viscosities around  $10^{24}$  Pa s, and stresses of  $\sim 100$  MPa. We find a strong dependence of global plate motions, trench rollback, net rotation, plateness, and strain rate on the stress exponent in the nonlinear viscosity; the yield stress is found to be important only if it is smaller than the ambient convective stress. Due to strong coupling between plates, slabs, and the surrounding mantle, the presence of lower mantle anomalies affect plate motions. The flow in and around slabs, microplate motion, and trench rollback are intimately linked to the amount of yielding in the subducting slab hinge, slab morphology, and the presence of high viscosity structures in the lower mantle beneath the slab. The lateral flow around slabs is generally trench-perpendicular, induced by the strongly

coupled downward motion of the subducting slabs, and therefore our models do not account for the trench-parallel flow inferred from shear-wave splitting analysis. Flow models before and after the plate reorganization around 50 Ma are not able to reproduce the rapid change in Pacific plate motion from northwest to west that is associated with the bend in the Hawaiian-Emperor chain, despite a nonlinear rheology and the incorporation of detailed reconstructed paleo plate boundaries and age grids. In these models at 55 and 45 Ma, slab age is an important factor in the slab pull, determining the coupling between plates and slabs and between upper and lower mantle sections of slabs. The overall dynamics appear to be dominated by the characteristics of slab remnants in the lower mantle. Subducting slabs affect lateral flow in the upper mantle on a much smaller scale, and therefore we conclude that it is unlikely that the slabs in the western Pacific are responsible for the slowing of sub-Pacific flow after the initiation of their subduction around 50 Ma.

# Contents

<b>Acknowledgements</b>	<b>iv</b>
<b>Abstract</b>	<b>vi</b>
<b>List of Figures</b>	<b>xi</b>
<b>List of Tables</b>	<b>xiii</b>
<b>1 Introduction</b>	<b>1</b>
1.1 Modeling Mantle Convection With Plates . . . . .	1
1.2 Parallel Adaptive Mesh Refinement . . . . .	3
1.3 Thesis Overview . . . . .	6
<b>2 Slab Stress and Strain Rate as Constraints on Global Mantle Flow</b>	<b>9</b>
2.1 Abstract . . . . .	9
2.2 Introduction . . . . .	10
2.3 Model Setup and Solution . . . . .	11
2.4 Results . . . . .	13
2.5 Discussion and Conclusions . . . . .	18
<b>3 Multi-Scale Dynamics and Rheology of Mantle Convection with Plates</b>	<b>22</b>
3.1 Abstract . . . . .	22
3.2 Introduction . . . . .	23
3.3 Methods . . . . .	27
3.3.1 Numerical Methods . . . . .	27
3.3.2 Model . . . . .	32
3.3.3 Model Analysis . . . . .	36



3.4	Results . . . . .	40
3.4.1	Introduction . . . . .	40
3.4.2	Plate Motions and Plateness . . . . .	44
3.4.3	Strain Rates . . . . .	58
3.4.4	State of Stress . . . . .	62
3.4.5	Regional Dynamics . . . . .	68
3.4.6	Model Quality . . . . .	77
3.5	Discussion . . . . .	80
3.6	Conclusions . . . . .	86
<b>4</b>	<b>Dynamics of the 50 Ma Plate Reorganization</b>	<b>87</b>
4.1	Abstract . . . . .	87
4.2	Introduction . . . . .	88
4.3	Methods . . . . .	92
4.4	Results . . . . .	97
4.4.1	Model Viscosity . . . . .	97
4.4.2	Plate Motions . . . . .	97
4.4.3	Surface State of Stress . . . . .	103
4.4.4	Slabs . . . . .	105
4.4.5	Lateral Mantle Flow . . . . .	111
4.5	Discussion . . . . .	113
4.6	Conclusions . . . . .	115
<b>5</b>	<b>Summary and Outlook</b>	<b>117</b>
5.1	Summary . . . . .	117
5.2	Outlook . . . . .	120
<b>A</b>	<b>Benchmarks</b>	<b>122</b>
A.1	Abstract . . . . .	122
A.2	Introduction . . . . .	123
A.3	Mantle Convection Equations . . . . .	125
A.4	Discretization and Solvers . . . . .	126
A.4.1	Variational Formulation of Stokes Equations . . . . .	126

- A.4.2 Boundary Terms and Topography . . . . . 128
- A.4.3 Stokes Solver . . . . . 130
- A.4.4 Advection-Diffusion Solver . . . . . 132
- A.5 Adaptivity . . . . . 134
  - A.5.1 Parallel Adaptive Meshes Based on a Forest of Octrees . . . . . 136
  - A.5.2 Handling of Nonconforming Meshes . . . . . 138
  - A.5.3 Criteria for Mesh Adaption . . . . . 144
  - A.5.4 Mesh Adaptation for Time-Dependent Problems . . . . . 146
- A.6 Tests and Benchmarks . . . . . 147
  - A.6.1 Analytical Solutions for the Stokes Equations . . . . . 147
  - A.6.2 Benchmarks for Stokes Solver . . . . . 152
  - A.6.3 Time-Dependent Benchmark . . . . . 158
  - A.6.4 Adaptive Resolution of Rising Plume . . . . . 159
- A.7 Discussion and Conclusions . . . . . 164

**Bibliography** **168**

# List of Figures

1.1	Splitting of the Earth's mantle into 24 warped cubes . . . . .	4
2.1	Plate motions and state of stress in the Bolivia region . . . . .	15
2.2	Plate motions and state of stress in the Tonga region . . . . .	17
2.3	Strain rate and stress in the Tonga and Bolivia slabs . . . . .	19
3.1	Map of regions and cross-sections selected for detailed analysis . . . . .	42
3.2	Cutouts of viscosity and the mesh in a global model through the Marianas and Philippines . . . . .	43
3.3	Global plate motions with variation of yield stress and stress exponent . . . . .	45
3.4	Schematic of the behavior of a resulting quantity as function of $(\sigma_y, n)$ . . . . .	47
3.5	Angle misfit, plate speed, and plateness constraints on global plate motions . . . . .	48
3.6	Pacific plateness with variation in yield stress and stress exponent . . . . .	50
3.7	Plate motions in NNR and hotspot reference frames . . . . .	51
3.8	Integrated viscosities in the upper mantle . . . . .	54
3.9	Net rotation as function of stress exponent and yield stress . . . . .	55
3.10	Plate motions and mantle viscosity for various lower mantle tomography conver- sion factors . . . . .	57
3.11	Comparison of surface strain rates . . . . .	60
3.12	Constraints for the strain rate in slabs . . . . .	62
3.13	Regional state of stress at the surface . . . . .	64
3.14	Cross-sections of the state of stress in slabs . . . . .	66
3.15	Variation of slab compression misfit with yield stress and stress exponent . . . . .	67
3.16	Variation of the amount of rollback $v_r$ with yield stress and stress exponent in several slabs . . . . .	71
3.17	Cross-sections through slabs and microplates . . . . .	73

3.18	Lateral flow at depth, plotted on viscosity . . . . .	76
4.1	Reconstruction of global plate motions between 60 and 45 Ma . . . . .	94
4.2	Reconstruction of plate motions in the western Pacific between 60 and 45 Ma . . . . .	95
4.3	Global cross-section through model viscosity . . . . .	98
4.4	Map view of modeled surface quantities; global view centered on the Pacific . . . . .	99
4.5	Map view of modeled surface quantities; zoom-in on the western Pacific . . . . .	101
4.6	Time evolution of global net surface rotation . . . . .	102
4.7	Map view of the surface state of stress, zoom-in on the western Pacific . . . . .	104
4.8	Cross-sections through subducting slabs at 55 Ma . . . . .	107
4.9	Cross-sections through subducting slabs at 45 Ma . . . . .	108
4.10	Outline of slabs on viscosity . . . . .	110
4.11	Map view of lateral mantle flow, zoom-in on western Pacific . . . . .	112
A.1	A 2D cartoon of an octree and the corresponding mesh . . . . .	136
A.2	Illustration of adaptive discretization of the mantle . . . . .	139
A.3	Illustration of a hanging face in a nonconforming adaptive discretization . . . . .	141
A.4	Globally unique node numbering and parallel sharer lists on an example mesh . . . . .	142
A.5	Interval-based adaptation over time . . . . .	147
A.6	Slice through the flow field for the exact ridge example solution . . . . .	153
A.7	Response functions for surface topography, CMB topography, velocity at the surface, and velocity at the CMB . . . . .	156
A.8	Errors in response functions for surface topography, CMB topography, velocity at the surface, and velocity at the CMB . . . . .	157
A.9	Temperature field at steady state for the time-dependent benchmark . . . . .	159
A.10	Measured quantities in time-dependent convection models with a temperature perturbation of degree 4 and order 0 . . . . .	160
A.11	Temperature field for plume models . . . . .	162
A.12	Measured quantities in plume model, for decreasing number of elements . . . . .	164

## List of Tables

3.1	Parameters used to nondimensionalize the mantle flow equations . . . . .	32
3.2	Parameters used in the viscosity law for the reference model . . . . .	36
3.3	Varied global rheology parameters . . . . .	41
3.4	Compilation of net rotation from several plate motion models and numerical models . . . . .	53
3.5	Table with model scores . . . . .	79
A.1	Errors for the polynomial solution example with constant viscosity . . . . .	150
A.2	Errors for the polynomial solution example with variable viscosity . . . . .	150
A.3	Errors for the ridge example . . . . .	152
A.4	Weak scaling for the mid-ocean ridge Stokes example . . . . .	154
A.5	Comparison of the time evolution of a rising plume on static uniform and dynamically adapted meshes . . . . .	161